Available online at www.sciencedirect.com
ScienceDirect
European Journal of Pharmaceutics and Biopharmaceutics 70 (2008) 345–356
European Journal of Pharmaceutics and Biopharmaceutics
www.elsevier.com/locate/ejpb

Research paper

Influence of crystal hydration on the mechanical properties of sodium naproxen

Etienne Joiris [a], Piera Di Martino [b,*], Ledjan Malaj [b], Roberta Censi [b], Christine Barthélémy [a], Pascal Odou [a]

[a] Galenic and Hospital Pharmacy Department, Lille, France
[b] Department of Chemical Sciences, University of Camerino, Camerino, Italy

Received 21 January 2008; accepted in revised form 15 April 2008
Available online 1 May 2008

Abstract

The aim of this work is to establish a correlation between water uptake by anhydrous sodium naproxen (ASN) at two different relative humidities and modifications in tableting and densification behaviour under hydration. Water uptake was evaluated at different relative humidities. Models for the hydration kinetics of ASN at 55% and 86%, corresponding to the formation of the dihydrated and tetrahydrated forms, respectively, were evaluated assuming Eyring's dependence on temperature. Tabletability, compressibility, compactibility, and densification behaviour were determined using an instrumented single punch tablet machine. Kinetic data are consistent with a model where water molecules enter the crystal preferentially along hydrophilic tunnels existing in the crystal structure and corresponding to the propionate side chain. Water inclusion perturbs the crystallographic structure, causing slight structural changes according to the amount and associated to an increase in entropy. The interposition of water molecules between sodium naproxen molecules weakens intermolecular bonds, and these sites can behave like sliding planes under compression. Such structural changes may explain the improved compression behaviour and modified densification propensity mechanism. Kinetic data describing the water hydration mechanism of ASN explain in an original way the improved tableting and densification properties under hydration.

Keywords: Sodium naproxen; Hydration; Kinetics; Tableting; Densification

1. Introduction

Naproxen ((*S*)-(+)-6-methoxy-α-methyl-2-naphtaleneacetic acid) is a drug belonging to the class of aryl propionic acid derivatives (APAD) of non-steroidal anti-inflammatory drugs (NSAID). It consists of an aromatic moiety and a propionate side chain, with an asymmetric carbon in the side chain [1]. Because of its low water solubility, sodium salt is preferred to its acidic form (Fig. 1).

Despite being a well-known drug, it has only recently been revealed that it can exist in several hydrated forms, when exposed to humid air. A dihydrated form of sodium naproxen was formed by exposing the powder to an RH higher than 55% [2], while a tetrahydrated one was formed at an RH higher than 76% [3].

Kim [4] has already described the monohydrated form of sodium naproxen, recovered by partially dehydrating the dihydrated form or by crystallising from a water–alcohol mixture. In addition, the same author also studied the dehydration mechanism of the dihydrated and monohydrated forms when heated [5,6].

Although there are many pharmaceutical ingredients, drugs or excipients capable of forming hydrates, few works have focused on explaining the effect of hydration on the mechanical properties of powders [7–9].

In a recent work [10], authors produced medicated granules of sodium naproxen by wet granulation in a high-shear

* Corresponding author. Department of Chemical Sciences, University of Camerino, Via S. Agostino, 62032 Camerino, Macerata, Italy. Tel.: +39 0737 402215; fax: +39 0737 637345.
E-mail address: piera.dimartino@unicam.it (P.Di Martino).

0939-6411/$ - see front matter © 2008 Elsevier B.V. All rights reserved.
doi:10.1016/j.ejpb.2008.04.012

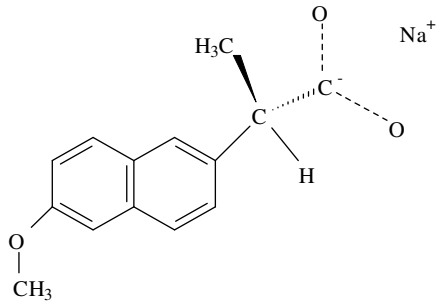

Fig. 1. Chemical structure of sodium naproxen.

mixer-granulator and verified that during the wetting phase sodium naproxen hydrated to the tetrahydrated form. By applying two different drying procedures, mixtures of different hydrated forms were recovered, and different compression behaviours described. To prove that differences in compression behaviour of sodium naproxen can be ascribed to hydration degree, the behaviour of the active raw material under compression will be examined at different hydration degrees in this work, the objective of this work is therefore double:

(a) To explore the mechanism of crystal hydration from anhydrous sodium naproxen to two different hydrated forms of sodium naproxen.
(b) To analyse the effect of hydration on the compression properties and densification mechanism of sodium naproxen powders.

Within this framework, authors will try to establish that a relationship exists between the hydration of sodium naproxen at different relative levels of humidity and its tableting and densification behaviour. The authors will also try to explain the reasons why differences in tableting and densification behaviour result from the mechanisms of water inclusion inside the crystal and the consequent perturbations caused by them.

2. Materials and methods

2.1. Chemicals

Anhydrous sodium naproxen (ASN) (Eur. Ph., USP) was kindly supplied by ACRAF (Ancona, Italy). To avoid unwanted hydration, ASN was stored in a desiccator in the presence of diphosphore pentaoxyde (Sigma–Aldrich, Stenheim, Germany). For the hydration experiments, several salts were used, capable of generating different relative humidity percentages (RH%): lithium chloride, potassium acetate, magnesium chloride, potassium carbonate, magnesium nitrate, ammonium nitrate, sodium chloride, ammonium sulfate, potassium chloride, and potassium sulfate (Sigma–Aldrich, Stenheim, Germany). During the compression study, Avicel PH 101 (FMC, Bruxelles, Belgium) and magnesium stearate (Mallinckrodt, Strasbourg, France) were used.

2.2. Isothermal water sorption experiments

Appropriate amounts of ASN were stored in an incubator (Velp Scientifica, FTC 90E, Usmate, Italy) at 25 °C. Powders were in turn placed in several boxes under appropriate RH%, obtained with saturated salt solutions, which generated a controlled water vapour pressure. Experimental RH% was checked with a thermohygrometer (Universal Enterprise Inc., Cambiago, Italy). Hydration was followed by a discontinuous procedure, i.e. by taking and weighing samples at regular intervals until reaching equilibrium weight [11]. Weight was checked every 10 days for three months. Assays were carried out in triplicate. Water uptake was calculated as a percentage of the initial mass of ASN. Sorption isotherms at 55% and 86% were established in the same experimental conditions, by weighing the samples twice daily. The powders recovered under hydration were used for the compression and densification study. The criteria for water uptake and water content were quite different because the mass of dried sample was used as reference in the first case, while the mass of humid product was used in the second. Target values are indicated in Table 1.

Powder water content was checked by thermogravimetry before compression (microbalance M3 and oven TG50, processor TC10, Mettler Toledo, France). Samples (2–3 mg) were heated from 25 to 125 °C at a heating rate of 10 °C/min under nitrogen atmosphere (10 ml/min) in aluminium oxide pans. Measures were carried out in triplicate. A blank assay was performed before each set of analyses.

The crystalline structure obtained during the hydration process was checked by powder X-ray diffractometry. For this purpose, a Philips PW 1730 (Holland) was used as X-ray generator for Cu Kα radiation (λ 1.54178 Å). Experimental X-ray powder patterns were recorded on a Philips PH 8203 apparatus, using a Philips PW 1373 goniometer and a Philips PW 1390 channel control. Data were collected in the step scan mode using a step size of 0.01° 2θ. The scanned range was 2° to 40° (2θ).

Table 1
Target values of water uptake and water content

Formula	Molecular weight	Water uptake (%)	Water content (%)
$C_{14}H_{13}O_3Na$	252	–	–
$C_{14}H_{13}O_3Na{\cdot}0.5H_20$	261	3.57	3.45
$C_{14}H_{13}O_3Na{\cdot}1.0H_20$	270	7.14	6.66
$C_{14}H_{13}O_3Na{\cdot}1.5H_20$	279	10.71	9.67
$C_{14}H_{13}O_3Na{\cdot}2H_20$	288	14.28	12.50
$C_{14}H_{13}O_3Na{\cdot}3H_20$	306	21.43	17.64
$C_{14}H_{13}O_3Na{\cdot}4H_20$	324	28.57	22.22

Table 2
Algebraic expressions corresponding to the most common mechanism generally used to describe changes in solid-state

Model	$g(\alpha)$	Mechanism (description of equation)
A2	$[-\ln(1-\alpha)]^{\frac{1}{2}}$	One-dimensional growth of nuclei (Avrami–Erofeyev equation, $n=2$)
A3	$[-\ln(1-\alpha)]^{\frac{1}{3}}$	Two-dimensional growth of nuclei (Avrami–Erofeyev equation, $n=3$)
A4	$[-\ln(1-\alpha)]^{\frac{1}{4}}$	Three-dimensional growth of nuclei (Avrami–Erofeyev equation, $n=4$)
R1	α	One-dimensional phase boundary reaction (zero-order mechanism)
R2	$1-(1-\alpha)^{\frac{1}{2}}$	Two-dimensional phase boundary reaction (contracting cylinder)
R3	$1-(1-\alpha)^{\frac{1}{3}}$	Three-dimensional phase boundary reaction (contracting sphere)
D1	α^2	One-dimensional diffusion
D2	$(1-\alpha)\ln(1-\alpha)+\alpha$	Two-dimensional diffusion
D3	$\left[1-(1-\alpha)^{\frac{1}{3}}\right]^2$	Three-dimensional diffusion (Jander's equation)
D4	$\left(1-\frac{2}{3}\alpha\right)(1-\alpha)^{\frac{2}{3}}$	Three-dimensional diffusion (Ginstling–Brounshtein equation)

2.3. Study of hydration kinetics

An experimental procedure similar to that previously described for the isothermal water sorption experiments was carried out to study hydration kinetics. The ASN powder was stored at two different RHs, 55% and 86%, at several temperatures (15, 20, 25, 30, and 35 °C) and generated in the appropriate saturated salt solutions. With the same discontinuous procedure as previously described, changes in weight were continuously and regularly checked until equilibrium was reached. The 55% and 86% RH values were used because they led, respectively, to the dihydrated form (DSN) [2] and the tetrahydrated form (TSN) [3].

To describe the process of water addition into the crystal, the following general equation was considered:

$$\frac{d\alpha}{dt} = k(T)\cdot f(\alpha) \tag{1}$$

where $k(T)$ is the rate constant at temperature T and α, the fractional degree of reaction represents the fraction of water added at time t, that is:

$$\alpha = \frac{M}{M_T} \tag{2}$$

where M is the mass of water in the sample at time t and M_T is the total mass of water in the sample at the end of hydration. The relationship between α and time is embodied in the function $f(\alpha)$, which in turn depends on the reaction model followed by water addition. Integration of Eq. (1) at constant temperature gives:

$$\int_0^1 \frac{d\alpha}{f(\alpha)} = g(\alpha) = \int_0^t k(T)\cdot dt = k(T)\cdot t \tag{3}$$

The rate constant $k(T)$ may be considered as follows, based on Eyring's dependence on T:

$$k(T) = \frac{k_B T}{h}\exp\left(\frac{\Delta S^*}{R}\right)\exp\left(\frac{-\Delta H^*}{RT}\right) \tag{4}$$

where ΔS^* is the activation entropy, ΔH^* is the activation enthalpy, R is the gas constant, k_B is the Boltzmann's constant, and h is the Planck's constant.

Both ΔS^* and ΔH^* can be estimated from rate constant values determined by isothermal measurements (at several temperatures), provided $g(\alpha)$ is known. Table 2 gives selected expressions [12,13] for $g(\alpha)$ corresponding to the most common solid-state processes. Plots were placed according to kinetic equations shown in Table 2 and their conformity assessed by the least-square method. The function that best fitted the hydration data was selected, and the corresponding values of k were determined. By fitting Eyring's expression to these values the activation enthalpy and entropy of the process could be determined.

2.4. Determination of particle shape and size

Particle shape and size were determined using a Scanning Electron Microscope (SEM) (Stereoscan 360, Cambridge Instruments, Cambridge, United Kingdom). Samples were mounted on a metal stub with a double-sided adhesive tape and then recovered under vacuum with a gold layer of thickness of 200 Å using a metallizer (Balzer MED 010, Linchestein). Particle size was determined by counting Ferret's diameter of 500 particles under SEM.

2.5. Study of compression properties

Compression was carried out in an instrumented single punch tablet machine (Frogerais OA, Vitry, France), equipped with flat punches of 11.28 mm in diameter.

Two sets of tablets were prepared for each powder. The powder mass was adapted so as to reach a maximal compression pressure of 150 ± 5 MPa (first set, to study tabletability and compressibility) or a porosity value of $10 \pm 0.1\%$ (second set, to study compactibility) [14,15]. Results are the mean of five measurements. The die depth was fixed at 10.00 mm and the upper punch displacement for an empty die at 7.50 mm. External lubrication was obtained by compressing microcrystalline cellulose along with 1% W/W magnesium stearate. For each tablet, an appropriate amount of powder was weighed and introduced manually into the die. The machine was started and measures were recorded at a frequency of 2000 Hz. The length of pressure application on the powder (compression and decompression) was about 150 ms. Once recovered, mass, thickness and crushing strength of tablet were measured, with scales (Precisa XT220 A), a microme-

ter (Mitutoyo, Japan) and a strength tester (Tablet Tester 8 M, Schleuniger, Switzerland), respectively. Correction of displacement transducer data for machine looseness and punch deformation was carried out according to Juslin and Paronen [16].

Pressure transmission through the powder bed in the die was estimated by comparing maximal compression pressures on the upper and lower punches. Transmission coefficient corresponds to the ratio of lower punch and upper punch values.

The densification behaviour of powders was studied using Heckel's equation [17]

$$\ln\frac{1}{1-D} = KP + A \tag{5}$$

where D is the relative density of the compressed powder bed at applied pressure P. K is the slope of the straight linear portion of Heckel's plot and the reciprocal of K is the mean yield pressure (P_y). The constant A is the sum of two densification terms

$$A = \ln\left(\frac{1}{1-D'_0}\right) + B \tag{6}$$

According to Doelker [18], D'_0 corresponds to the relative density of the powder at the moment when the last recorded applied pressure is still nil, and B' is the densification due to particle fragmentation. Constants A and B' can be expressed as relative densities using

$$D_A = 1 - e^{-A} \tag{7}$$

$$D'_B = D_A - D'_0 \tag{8}$$

Heckel's profiles were established from single compression cycles on tablets compressed approximately at 150 MPa. Parameters P_y, D_A, D'_0, and D'_B were calculated using a pre-compression pressure value of 2.0 MPa. Several methods have been described to select a linear region of the Heckel function in order to determine Heckel constants. Following Paronen and Ilkka [19], we selected a range of measurement points where the linear regression coefficient was as high as possible. This corresponded for both samples to the 50–100 MPa range, with coefficient values superior to 0.998. Each value is a mean of five measurements.

Total elastic recovery (ER) was calculated according to Armstrong and Haines-Nutt [20]:

$$\mathrm{IER} = \left[\frac{(t_2 - t_1)}{t_1}\right] \times 100 \tag{9}$$

where t_1 is the minimal thickness of the powder bed in the die and t_2 is tablet thickness.

Tablet porosity (ε) was calculated from weight, volume and apparent powder density. Minimal porosity (ε_{min}) refers to powder porosity when maximal compression force was applied during each compression cycle. It was determined from weight, die dimensions and apparent powder density using a helium pychnometer (Accupic 1330, Micromeritics, Norcross, USA), with a cell of 10 cm^3. Results are the mean of 10 measurements. Densities of ASN, DSN, and TSN were, respectively, 1.377 ± 0.008, 1.343 ± 0.006, and 1.337 ± 0.005. The density of intermediate hydrates was calculated by averaging apparent powder densities as a function of water content.

Crushing force was measured immediately after compression with a tablet strength tester (Erweka, type TBH30, Germany). Tensile strength Q [21] was calculated according to

$$Q = \frac{2H}{\pi \times d \times t} \tag{10}$$

3. Results

3.1. Isothermal water sorption experiments

Results of isothermal water sorption experiments on ASN at 25 °C are given in Fig. 2. For relative humidity (RH) lower than 55%, water uptake was very low after 10 days of exposure. A weight increase corresponding to two water molecules for one ASN molecule was noted. This was followed by a rather short plateau, then a second water uptake corresponding to two additional water molecules at 76% RH, and finally by a plateau above 76% RH. These results concord well with those of Di Martino et al. [3]. The first plateau corresponds to the formation of dihydrated sodium naproxen (DSN), while the second one cor-

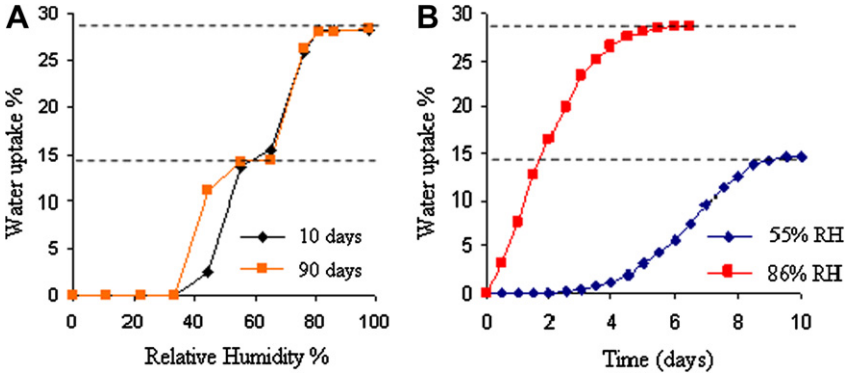

Fig. 2. Sodium naproxen water uptake expressed versus relative humidity % (A) and versus time (B).

responds to that of tetrahydrated sodium naproxen (TSN). It should be noted that the curve obtained after 90 days at different RH% is identical, with the exception of the dot at 43%, where water uptake considerably increased with time due to the slow formation of the dihydrated form at this RH% value. This phenomenon was previously described by Kontny and Zografi [11] for other hydrated systems. The kinetics of water uptake at 25 °C at RHs of 55% and 86% are given in Fig. 2b. At 55%, DSN formation required a latency period of some days. At 86%, TSN formation started immediately and was more rapid. These curves were used to prepare the samples for tableting experiments. Powders under hydration were checked by XRPD. These analyses showed that, at an RH of 55%, when water uptake was not still complete, powders were composed of a mixture of ASN and DSN, without any intermediate crystalline form, such as, for example, monohydrate sodium naproxen (MSN). This result is clearly shown in Fig. 3a, where XRPD patterns of sodium naproxen exposed to 55% RH are presented when hydration was at 50%, as well as those of ASN, the starting material, and DSN, the completely hydrated form. The intermediate form is clearly composed of a mixture of the two pure forms (ASN and DSN), and no peaks of any other forms, such as MSN, were visible. Peak intensities are proportional to water sorption and results concord with the previously published data [3], showing that typical ASN peaks progressively decrease as DSN peaks appear, without any other different forms. Similarly, at an RH of 86%, when water uptake was not still complete, powders were composed of a mixture of ASN and TSN, without any intermediate crystalline form such as, for example, MSN or DSN, as can be seen in Fig. 3b. These results concord with those of Di Martino et al. [3].

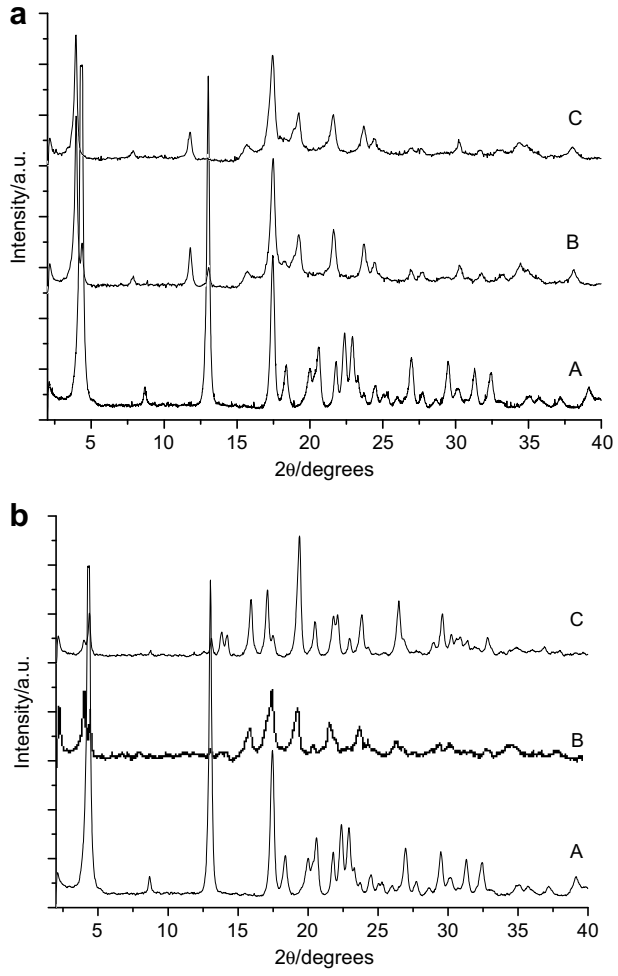

Fig. 3. XRPD patterns of powders under hydration. (a) ASN starting material (A), after 6 days of exposure to 55% RH (50% hydration) (B), and completely hydrated DSN powder (C). (b) ASN starting material (A), after 2 days of exposure to 86% RH (50% hydration) (B), and completely hydrated TSN powder (C).

Fig. 4 shows the particle morphology of ASN, the starting material, and of the completely hydrated and now pure forms, DSN and TSN. This evaluation, together with particle size, is important particularly afterwards, when interpreting compression and densification behaviour. Particles are irregular with smoothed edges; there are no obvious differences between the three products and hydration does not seem to affect particle morphology.

Particle sizes and distributions are given in Fig. 5. No differences occurred as a consequence of hydration, and slight variations among the three products are not statistically relevant.

3.2. Study of hydration kinetics

Table 3 and Fig. 6 give the results of ASN hydration at two different relative levels of humidity and at different temperatures. At 55% RH, reaction was in three stages (Fig. 6a). The induction period of nucleation, which is the initial reaction step, was rather long in time, but insignificant in weight increase. During the subsequent stage at the interface, i.e. the acceleratory period, weight increased with time, and this was followed by a decay period. The experimental M versus t curves had a sigmoid shape. Values suggest that hydration proceeded according to the model reported in Table 3. In the present case, such curves could only fit one of the models reported in Table 2, and so fitting was performed separately for the induction period and for the acceleratory-decay period. The first hydration period involved a D1 model, i.e. one-dimensional diffusion. When a gas molecule is fixed to a solid substratum, the ΔS^* should be negative, because the gas molecule loses degrees of translation freedom. However, a positive and non-negligible ΔS^* was obtained during the induction period, meaning that the freedom degrees of the activated state compensated for the loss of freedom degrees by water. Enthalpy value (ΔH^*) was high, suggesting that introduction of the water molecule greatly modified the rigid structure of the crystal. Eyring's parameters suggest that the entry of the water molecule alters the crystalline form towards a more expanded structure, in which the hydrated solid has more freedom degrees than the anhydrous one.

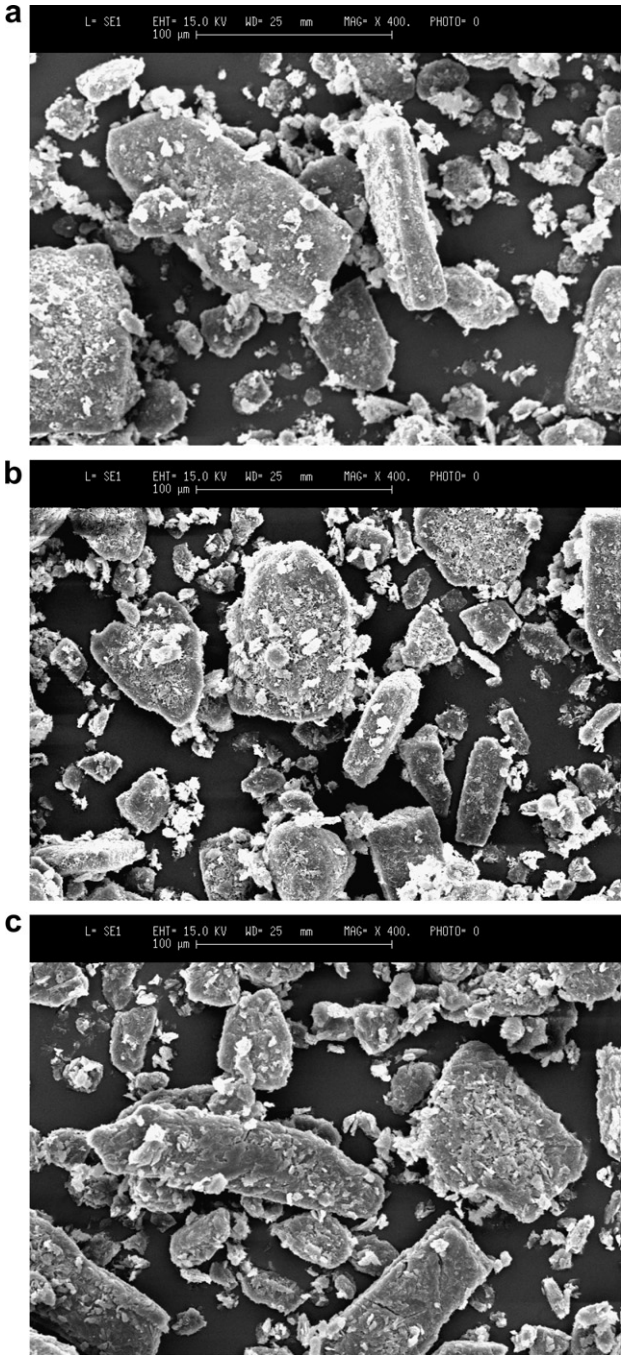

Fig. 4. SEM microphotographs of ASN (a), completely hydrated DSN after exposure to 55% RH (b), and completely hydrated TSN after exposure to 86% RH (c).

The second stage of the hydration reaction is best described by an A2 model (Avrami–Erofeyev equation, $n = 2$), which indicates that reaction is controlled by one-dimensional growth of nuclei. ΔS^* (-332.7 J K^{-1} mol^{-1}) was now negative and reflected the expected entropy loss of water molecules entering the solid. On the other hand, the enthalpy change ($\Delta H^* = 5.0$ kJ mol^{-1}) was much lower than during the induction period, suggesting that there was little enthalpic hindrance to the growth of the new phase.

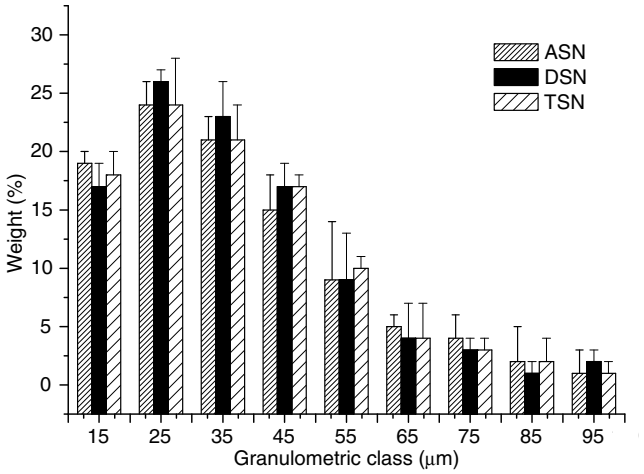

Fig. 5. Particle size and distribution of sodium naproxen particles. ASN, anhydrous sodium naproxen; DSN, dihydrated sodium naproxen; TSN, tetrahydrated sodium naproxen.

To sum up, the hydration process for ASN exposed to 55% RH occurred in two steps: firstly, water molecules diffused inside the crystal, accessing through hydrophilic sites present in the crystal (first step corresponding to the D1 model) and then water reacted with surrounding SN molecules to create new bonds and rearrange molecules (second step corresponding to the A2 model).

A rather different reaction model is involved when the solid is exposed to 86% RH (Table 3 and Fig. 6b). In this case the induction period, if any, was no more than a few hours, i.e. shorter than the time interval chosen for the experimental design. Two different reaction models gave a very good fit for $g(\alpha)$ versus t: (a) the one-dimensional growth of nuclei (Avrami–Erofeyev equation, $n = 2$), i.e. the same involved in the second stage of hydration at 55% RH and (b) the two-dimensional phase boundary reaction (contracting cylinder, R2 model). The ΔS^* values for the two models, both negative and quite similar to each other, were similar to that found for the second hydration stage at 55% RH. Also the ΔH^* values were quite similar to each other (respectively, 24.1 or 22.0 kJ mol^{-1}), but higher than the value found for the second hydration stage at 55% RH. Then at 86% RH, when four water molecules rather than two entered the lattice, hydration was accompanied by a greater enthalpy change, probably due to more notable crystallographic changes.

To sum up, and by analogy with hydration results at 55% RH, the R2 model (two-dimensional phase boundary reaction) seems the most probable mechanism, because again it implies water diffusion through pre-existing hydrophilic channels, then the association of water with polar groups capable of forming hydrogen bonds with water.

3.3. Compression behaviour

Before compression all the hydrated powders were analysed by TGA to verify whether hydration occurred as

Table 3
Eyring's parameters for hydration process

Hydration condition	Model	T (°C)	K (s^{-1})	r	Eyring plot		
					ΔH^* (kJ mol^{-1})	ΔS^* (J K^{-1} mol^{-1})	r
55% RH first step	D1	15	7.590×10^{-9}	0.942	122.4	+30.8	0.910
		20	9.780×10^{-8}	0.947			
		25	9.722×10^{-8}	0.898			
		30	1.886×10^{-7}	0.970			
		35	3.670×10^{-7}	0.950			
55% RH second step	A2	15	3.05×10^{-6}	0.978	5.0	−332.6	0.999
		20	3.12×10^{-6}	0.984			
		25	3.21×10^{-6}	0.965			
		30	3.37×10^{-6}	0.974			
		35	3.65×10^{-6}	0.992			
86% RH	A2	15	2.88×10^{-6}	0.996	24.1	−266.5	0.992
		20	3.69×10^{-6}	0.998			
		25	4.51×10^{-6}	0.996			
		30	5.06×10^{-6}	0.994			
		35	6.06×10^{-6}	0.989			
86% RH	R2	15	1.39×10^{-6}	0.997	22.0	−280.2	0.997
		20	1.69×10^{-6}	0.995			
		25	2.02×10^{-6}	0.996			
		30	2.27×10^{-6}	0.988			
		35	2.75×10^{-6}	0.985			

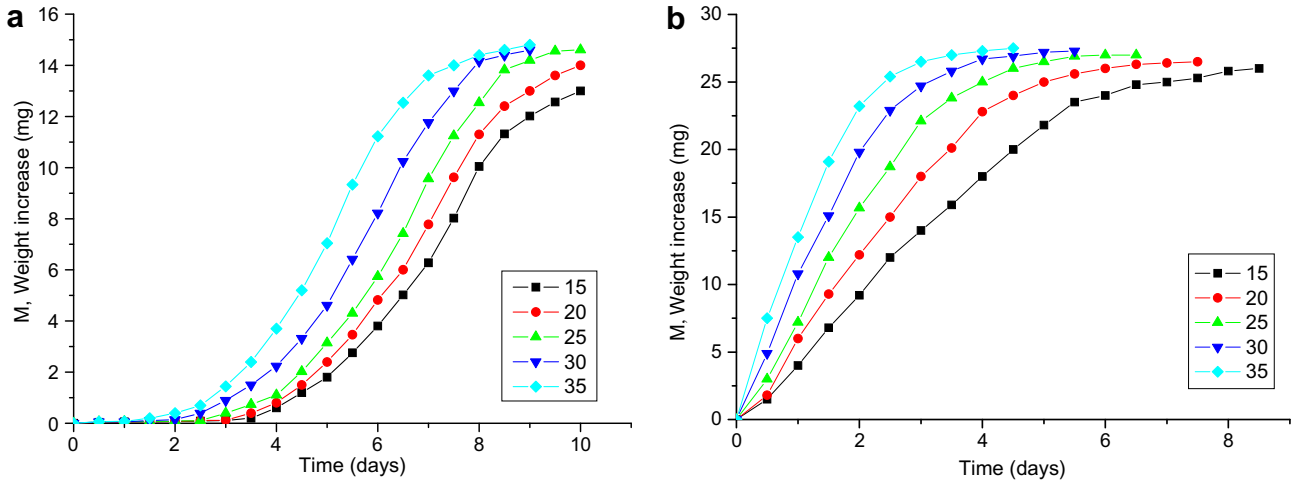

Fig. 6. Sodium naproxen hydration rate at different experimental temperatures. (a) NS exposed to 55% RH; (b) NS exposed to 86% RH.

expected. It should be noted that in the case of sodium naproxen TGA does not make it possible to distinguish between bound and absorbed water. This fact has also been previously highlighted by Kim [6] and Di Martino et al. [2] and is due to the fact that the loss of bound water starts at quite low temperatures close to those favouring the loss of absorbed water.

All the tested products showed very favourable behaviour under compression and no capping, sticking or seizing problems arose during this study.

Results are given in Fig. 7a (tabletability), b (compressibility), and c (compactibility). In these figures, the unit used to represent the amount of water is the mean stoichiometric coefficient (MSC), that is, the number of water molecules per molecule of SN. It is of paramount importance to keep in mind that this number is a mean number, because hydrates in formation are the mixtures of anhydrous and hydrated forms, and not intermediate hydrates.

The tabletability of ASN was relatively good. The tensile strength after compression at 150 MPa was 1.25 MPa. The values for the hydrated forms were higher: 2.59 MPa for DSN and 3.30 MPa for TSN. Tensile strength of hydrates in formation was proportional to MSC (Fig. 7a). At 55%, the progressive formation of DSN corresponded to a progressive increase in tablet resistance, indicating a very significant correlation between tabletability and water content. At 86%, the progressive formation of TSN yielded a bell trend, with a maximal tensile strength of 3.95 MPa for an MSC of 3. Beyond this point, the increase in water content corresponded to a

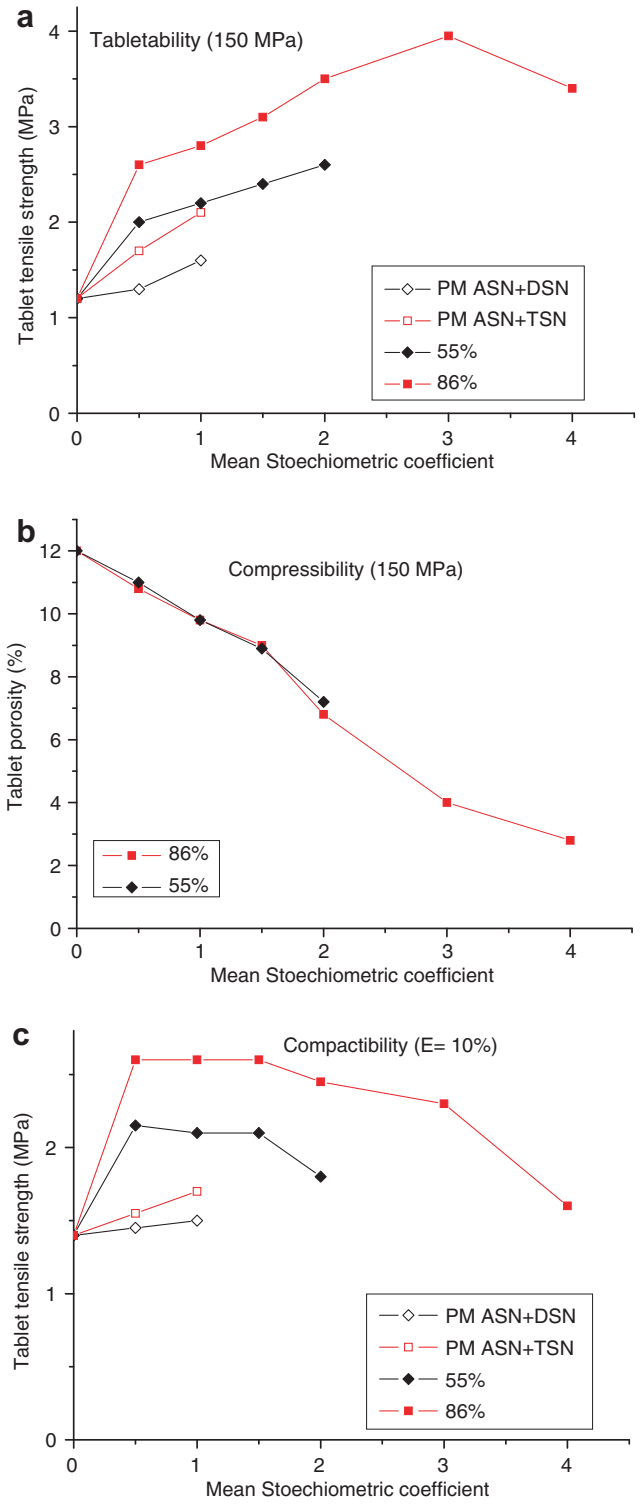

Fig. 7. Tabletability (a), compressibility (b), and compactibility (c) of SN hydrated forms. Each point is the mean of five independent determinations and is given with the 95% confidence interval. Solid symbols correspond to hydrates in formation at 55% (blue) and 86% (red). The open symbols correspond to the physical mixtures of ASN and DSN (blue) and ASN and TSN (red). (For interpretation of the references to colour in this figure legend, the reader is referred to the web version of this paper.)

decrease in tensile strength. The compression behaviour of hydrated samples was compared to that of physical mixtures (PM) prepared by gently mixing different proportions of pure ASN and DSN or pure ASN and TSN in a mortar. Compression of physical mixtures of ASN and DSN (ASN:DSN of 75:25 or 50:50), or ASN and TSN (ASN:TSN 12.5:87.5 and 75:25), corresponding to MSCs of 0.5 and 1, was then carried out. For the same water amount, the tabletability of physical mixtures was lower than that of hydrates in formation. It is clear that the way in which water is distributed among the particles is fundamental. In the case of physical mixtures, water is present in one portion of particles, while the other portion is anhydrous. However, in hydrates in formation, the water involved in hydration may be assembled in the periphery of particles, while the centre remains dry. This phenomenon is compatible with the typical structure of " channel hydrates" [22]. Kim [4] observed a similar situation under optical microscopy, but the other way round, during the dehydration of MSN to ASN: there was initial dehydration at the periphery of the particles followed by progression of the phenomenon to the centre of the crystal parallel to the channels.

To have a better understanding of the profiles of tabletability, other representations are required. Tablets can be considered as the dispersion of particles in the air. Their cohesion comes from the intermolecular strength among particles that can act only when distances are very small [23]. Any variation in tablet cohesion can thus theoretically be caused either by a modification of interparticle distances or by an alteration in the intensity and/or the number of bonds. These phenomena can be explained by interpreting the compressibility and compactibility results.

Water greatly modifies the compressibility of SN. After compression at 150 MPa, tablet porosity changes from 12.1% for ASN to 7.2% for DSN and 2.4% for TSN. The compressibility of hydrates in formation is presented in Fig. 7b. The porosity of tablets produced at 150 MPa progressively decreases as a function of water content. This porosity reduction is comparable, whatever the water uptake, at 55% or 86%. Pearson's test carried out on the data shows that a very good correlation exists between tablet porosity and MSC ($r = -0.97$, $p < 0.0001$). Compressibility data of physical mixtures are not presented in the same figure, because it is exactly superposed over that of hydrates in formation. These results show that SN particles are closer together in water for the same compression pressure. The tabletability of SN is therefore increased by the presence of water. However, such evidence is inadequate to explain the differences observed between DSN and TSN, between hydrates in formation and those between physical mixtures and the bell profile of the tabletability of TSN. This is the reason why it is also essential to consider compactibility, which makes an assessment of the strength of interparticle bonds possible. The basic concept for a compactibility study is to make and compare the mechanical resistance of tablets of the same porosity for any substance under study. As proximity between particles is the same, the differences observed can be attributed to

the number and/or intensity of interparticle bonds. For this study therefore, new tablets must be produced and porosity fixed at 10%, a value at which it is possible to recover tablets for any powder under study. The tensile strengths are 1.45, 1.83, and 1.77 MPa, respectively, for ASN, DSN, and TSN at 10% porosity. As these values are quite close, they are not very informative and so the complete profiles of hydrates in formation and of physical mixtures are given in Fig. 7c. It can be observed that for the very first water content tested (MSC 0.5), the compactibility of DSN and TSN in formation abruptly increased to reach the values of 2.18 and 2.57 MPa, respectively. These values changed little as water content increased, giving the profile of compactibility as a plateau. The last value on each curve (corresponding to DSN and TSN completely formed) was significantly lower, and more pronounced for TSN. In addition, the evolution of compactibility for physical mixtures was completely different and remained intermediate between the values measured for ASN and complete hydrates. All this information is compatible with a hydration model in which water enters into the anhydrous particles through pre-existing channels and thus remains confined at the periphery of the crystals, causing an abrupt modification to particle surface and thus to interparticle bonds. The higher compactibility of TSN in formation compared to DSN may account for its better tabletability. It must be considered that the tetrahydrated form can already be formed at lower RH% (up to 64%) as proven by water sorption isotherms. Exposure to higher humidity levels (as in the case of 86% RH) can imply that a part of the water is involved in the hydration of the crystal (to form the tetrahydrated structure) and excess water is absorbed inside the tunnels and on the crystal surface. Consequently, it is possible to assume that at the end of hydration, when the crystalline structure is "saturated", the available water is adsorbed on the surface of the particles, covering them with a thin film that reduces the possibility of interparticle bonds. However, as it is impossible to quantify exactly the water absorbed by TGA, as previously explained, this can only be a supposition. Water distribution in physical mixtures is completely different, yielding samples of lower compactibility than that of hydrated forms and practically uninfluenced by mixture composition.

3.4. Densification mechanism

The study of the compression behaviour of SN showed that hydration water significantly increased compressibility. The objective of the densification study is to obtain information about the mechanisms related to compressibility changes.

The first step in the study was to identify in which phase (compression or decompression) the compressibility modifications due to hydration take place. Fig. 8 shows the effect of hydration on the minimal porosity of tablets in formation, at the end of compression phase (Fig. 8a),

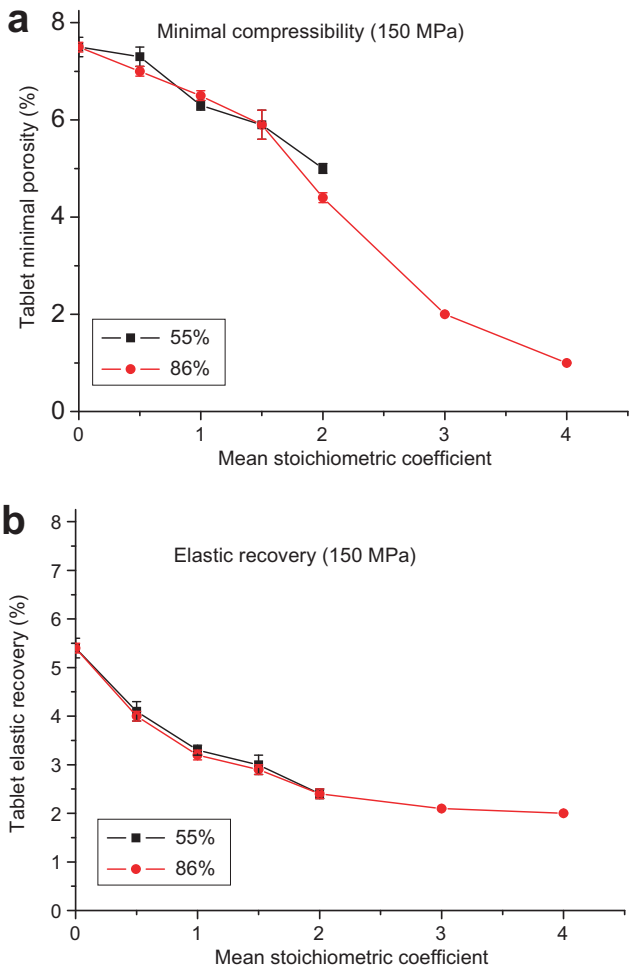

Fig. 8. Minimal porosity (a) and elastic recovery (b) expressed versus MSC. Each point is the mean of five independent determinations and is given with the 95% confidence interval. Solid symbols correspond to hydrates in formation at 55% (blue) and 86% (red). The open symbols correspond to the physical mixtures of ASN and DSN (blue) and ASN and TSN (red). (For interpretation of the references to colour in this figure legend, the reader is referred to the web version of this paper.)

and on the elastic recovery of tablets during decompression. Results are given in Table 4. These results clearly show that two different mechanisms contribute to the increase in compressibility. When hydration starts, minimal porosity changes little, while elastic recovery decreases. Afterwards, minimal porosity decreases while elastic recovery levels off at a low value. The limit between these two phases is located at a stoichiometric coefficient of 1.5. It is visible in Fig. 8b which presents the whole evolution of compressibility. Results corresponding to the same MSC are similar, whether water uptake is at 55% or 86%.

The second step in the densification study focuses on the way the particle is deformed during the compression phase. This is done by analysing the parameters of Heckel's equation (Table 4). These values show that ASN particles fragment during compression (high D'_B and P_y) and that they change progressively during hydration, indicating a modification in the densification mechanism, from fragmentation

Table 4
Compressibility values and Heckel's parameters, expressed with their 95% confidence intervals, of tablets produced at 150 MPa

HR (%)	CSM	ε (%)	ε_{min}(%)	RE (%)	P_y (MPa)	D'_0	D'_B
55	0	12.1 ± 0.3	7.4 ± 0.3	5.30 ± 0.19	125.1 ± 0.9	0.583 ± 0.002	0.186 ± 0.002
	0.5	10.9 ± 0.3	7.2 ± 0.3	4.12 ± 0.17	113.4 ± 0.9	0.552 ± 0.003	0.179 ± 0.002
	1	9.4 ± 0.2	6.3 ± 0.2	3.44 ± 0.06	104.0 ± 1.0	0.576 ± 0.001	0.152 ± 0.001
	1.5	8.5 ± 0.2	5.7 ± 0.3	3.12 ± 0.08	97.8 ± 0.1	0.584 ± 0.006	0.136 ± 0.006
	2	7.2 ± 0.3	5.0 ± 0.1	2.39 ± 0.05	92.9 ± 1.0	0.605 ± 0.002	0.120 ± 0.001
86	0	12.1 ± 0.3	7.4 ± 0.3	5.30 ± 0.19	125.1 ± 0.9	0.583 ± 0.002	0.186 ± 0.002
	0.5	10.5 ± 0.2	6.9 ± 0.1	4.02 ± 0.20	110.1 ± 0.6	0.566 ± 0.002	0.161 ± 0.001
	1	9.5 ± 0.2	6.5 ± 0.2	3.34 ± 0.09	106.6 ± 1.6	0.572 ± 0.002	0.149 ± 0.003
	1.5	8.7 ± 0.3	5.7 ± 0.4	3.00 ± 0.10	99.4 ± 2.2	0.582 ± 0.004	0.137 ± 0.004
	2	6.6 ± 0.3	4.4 ± 0.2	2.35 ± 0.10	87.3 ± 2.3	0.585 ± 0.003	0.132 ± 0.005
	3	3.8 ± 0.2	1.9 ± 0.1	1.98 ± 0.15	61.4 ± 2.8	0.609 ± 0.003	0.131 ± 0.007
	4	2.4 ± 0.2	0.7 ± 0.2	1.80 ± 0.28	47.6 ± 2.0	0.642 ± 0.003	0.162 ± 0.006

Each value is the mean of five independent determinations.
MSC, MSC; ε, tablet porosity; ε_{min}, minimal porosity; P_y, mean yield pressure.

to plastic deformation (lower P_y). With TSN the peculiarity is the association of a high D'_B value to a low P_y, corresponding to the high compressibility of this product. Results registered during this second part of the work are similar for the common stoichiometric coefficients, independently of the RH% used for water uptake (55% or 86%).

Results of the densification study are confirmed by examining the general profiles of Heckel's cycles. The cycles obtained for tablets produced at the same final porosity of 10% are given in Fig. 9. For low water content, the decrease in the initial curve is clearly evident, and corresponds to the change from volume reduction by fragmentation to plastic deformation. The decrease in elastic recovery is also clearly evident, as can be noted by the decompression phase which becomes more horizontal. For the highest water content, the increased slope in the climbing part of the cycle can be observed with maximal pressure, which becomes weaker and weaker to obtain tablets of 10% porosity.

Modification in the densification mode is at the origin of the tabletability and compactibility improvement to be seen at the very start of hydration. Indeed, as explained above, the water captured at the initial phase of hydration may be concentrated in the periphery of the crystal. This external zone can become highly deformable, increasing the interparticle contact surface. This hypothesis is compatible with the fact that TSN, which is more plastic than DSN, also displays greater compactibility.

4. Discussion

4.1. Relationship between hydration and the mechanical properties of SN

The crystallographic structure of naproxen acid has been described as monoclinic [24,25] and the presence of the Na atom in the salified form does not modify this [26]. The Na atom participates in an "O···Na" type interaction, where Na is simultaneously linked to four oxygen

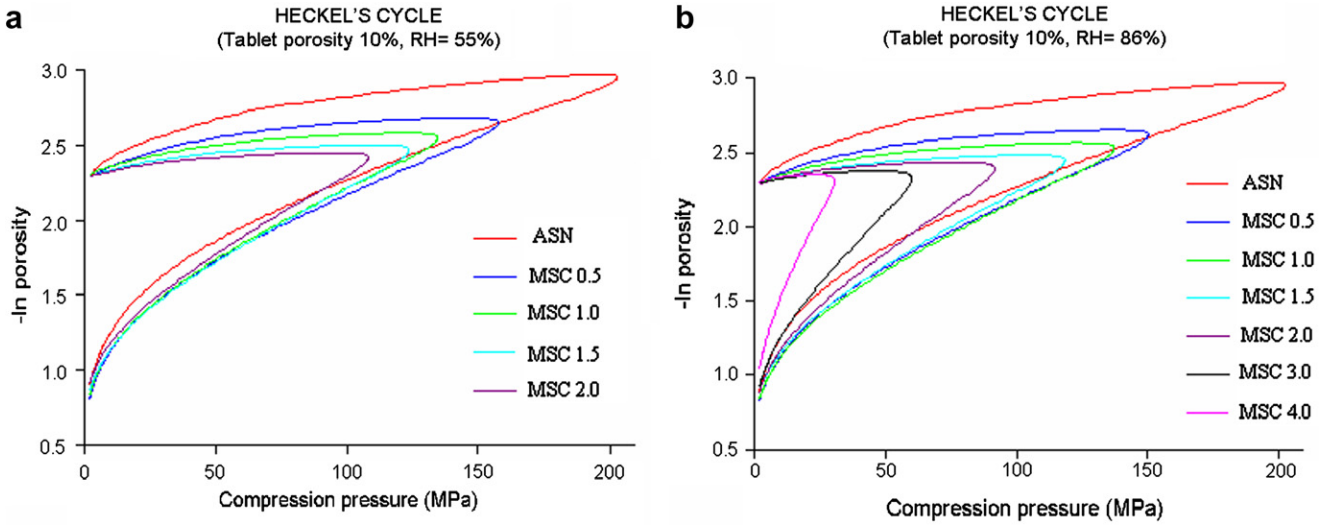

Fig. 9. Heckel's cycles for tablets of 10% porosity. Tablets are produced from SN under hydration at 55 (a) and 86% (b) RH. Each curve corresponds to whole values recorded while producing one tablet.

atoms forming a tetramer that stabilises the structure [26]. Di Martino et al. [2,3] have classified the hydrated forms of SN as "channel hydrates" according to Morris [22]. During the hydration process, water molecule access into the crystal is limited by the presence of some hydrophobic sites, mainly formed by the π cloud of the naphthalene rings. Water molecules can thus move preferentially from the periphery of the crystals along hydrophilic tunnels existing in the crystal structure and corresponding to the propionate side chain. Water molecules can then be easily accommodated between the SN molecules by forming hydrogen bonds with both Na and/or O atoms. The dimensions of the tunnel can be dependent on the number of water molecules placed in the tunnel (two for the dihydrated and four for the tetrahydrated). The conformational changes associated with hydration promote crystallographic modifications. Consistently with this, hydrated forms of sodium naproxen can be considered as "expanded channel hydrates" [22]. In this hydrated form, the water molecules converge on channels in the crystal structure, causing the distance between some crystalline planes to be increased proportionally to the amount of water. In this kind of structure, the water molecules are mainly bound together by hydrogen bonds and interact little with the host molecule. Thus, water molecules can easily move into the channel, bringing about easy and progressive hydration or dehydration of the crystals. This can explain the progressive increase in plastic deformation of hydrated forms which is proportional to the increase in water inside the crystal, as well as the modification in the densification mechanism from fragmenting to plastic deformation. This also accounts for the differences between the dihydrated and tetrahydrated forms. The intermolecular spaces occupied by water molecules behave like "sliding planes" for plastic deformation. In a previous study, Sun and Grant [15] explained the greater tableting propensity of the monohydrated form of *p*-hydroxybenzoic acid in its anhydrous form through the combination of a larger interparticle bonding area, thanks to the presence of water, and higher bonding strength. In fact, in the monohydrated form, the water molecules fill the spaces between the layers and facilitate the plastic deformation of the crystals by maintaining a larger separation between the zigzag-shaped planes.

5. Conclusion

This study clearly shows that hydration considerably changes the compression behaviour of SN. The insertion of the water molecule into the crystal modifies the tabletability, compressibility and compactibility of SN. However, the effect is not always proportional to water content. The complex evolution of tabletability, which is the main property for the industrial production of tablets, can be explained by considering the evolution of both compressibility and compactibility. It has been supposed that the water penetrating into the crystal is localised in the periphery. The kinetic study explaining how water enters into the crystal offers a better understanding of why the hydrated forms of SN show better tabletability than the anhydrous one.

The results of this work are relevant to industrial practice as they can orient choice towards the most appropriate form of sodium naproxen as a raw material for industrial tablet production and support the preparation of tablets by direct compression at lower costs and with improvements in biopharmaceutical properties.

Acknowledgement

Authors thank Alexandra Tavernier (M.A. University of Glasgow; Professeur Agrégée, University of Lille) for her kind help in revising the English manuscript. Authors dedicate this work to their dear colleague, Prof. Etienne Joiris, whose premature death occurred during the writing of this manuscript.

References

[1] Y. Kim, D. VanDerveer, A.P. Wilkinson, R.W. Rousseau, Anhydrous sodium naproxen, Acta Crystallogr. E60 (2004) m419–m420.
[2] P. Di Martino, C. Barthélémy, G.F. Palmieri, S. Martelli, Physical characterization of naproxen sodium hydrate and anhydrate forms, Eur. J. Pharm. Sci. 14 (2001) 293–300.
[3] P. Di Martino, C. Barthélémy, E. Joiris, D. Capsoni, A. Masic, V. Massarotti, R. Gobetto, S. Martelli, M. Bini, A new tetrahydrated form of sodium naproxen, J. Pharm. Sci. 96 (2007) 156–167.
[4] Y.S. Kim, Crystallization and solid-state transformations of the pseudopolymorphic forms of sodium naproxen, Ph.D. Thesis, Georgia Institute of Technology, Atlanta, 2005.
[5] Y.S. Kim, R.W. Rousseau, Characterization and solid-state transformations of the pseudo-polymorphic forms of sodium naproxen, Crystal Growth Des. 4 (2004) 1211–1216.
[6] Y. S Kim, H.S. Paskow, R.W. Rousseau, Propagation of solid-state transformations by dehydration and stabilization of pseudopolymorphic crystals of sodium naproxen, Crystal Growth Des. 5 (2005) 1623–1632.
[7] C.F. Lerk, K. Zuurman, K. Kussendrager, Effect of dehydration on the binding capacity of particulate hydrates, J. Pharm. Pharmacol. 36 (1983) 399.
[8] D.Y.T. Wong, P. Wright, M.E. Aulton, The deformation of alpha-lactose monohydrate and anhydrous alpha-lactose monocrystals, Drug Dev. Ind. Pharm. 14 (1988) 2109–2126.
[9] C. Sun, D.J.W. Grant, Improved tableting properties of *p*-hydroxybenzoic acid by water of crystallization: a molecular insight, Pharm. Res. 21 (2004) 382–386.
[10] P. Di Martino, L. Malaj, R. Censi, S. Martelli, Physico-chemical and technological properties of sodium naproxen granules prepared in a high-shear mixer-granulator, J. Pharm. Sci. (2008), doi:10.1002/jps.21400.
[11] M.J. Kontny, G. Zografi, Sorption of water by solids, in: H.G. Brittain (Ed.), Physical Characterization of Pharmaceutical Solids, Marcel Dekker, New York, 1995, pp. 387–418.
[12] J. Šesták, B. Gunnar, Kinetics of the mechanism of solid-state reactions at increasing temperature, Thermochim. Acta 3 (1971) 1–12.
[13] Z. Dong, J.S. Salsbury, D. Zhou, E.J. Munson, S.A. Schroeder, I. Prakash, S. Vyazovkin, C.A. Wight, D.J.W. Grant, Dehydration kinetics of neotame monohydrate, J. Pharm. Sci. 91 (2002) 1423–1431.
[14] E. Joiris, P. Di Martino, C. Berneron, A.-M. Guyot-Hermann, J.C. Guyot, Compression behaviour of orthorhombic paracetamol, Pharm. Res. 15 (1998) 1122–1130.

[15] C. Sun, D.J.W. Grant, Influence of crystal structure on the tableting properties of sulfamerazine polymorphs, Pharm. Res. 18 (2001) 274–280.
[16] M.J. Juslin, T.P. Paronen, On the accuracy of displacement measurements by instrumented single-punch machine, J. Pharm. Pharmacol. 32 (1980) 796–798.
[17] R.W. Heckel, Density–pressure relationships in powder compaction, Trans. Metall. Soc. AIME 221 (1961) 661–675.
[18] E. Doelker, Assessment of powder compaction, in: D. Chulia, M. Deleuil, Y. Pourcelot (Eds.), Powder Technology and Pharmaceutical Process, Elsevier, Amsterdam, 1994, pp. 403–471.
[19] P. Paronen, J. Ilkka, Porosity-pressure functions, in: G. Alderborn, C. Nyström (Eds.), Pharmaceutical Powder Compaction Technology, Marcel Dekker, New York, 1996, pp. 55–75.
[20] N.A. Armstrong, R.F. Haines-Nutt, Elastic recovery and surface area changes in compacted powder systems, Powder Technol. 9 (1974) 287–290.
[21] J.T. Fell, J.M. Newton, Determination of tablet strength by the diametral-compression test, J. Pharm. Sci. 5 (1970) 688–691.
[22] K. Morris, Structural aspect of hydrates and solvates, in: H.G. Brittain (Ed.), Polymorphism in Pharmaceutical Solids, Marcel Dekker, New York, 1999, pp. 125–181.
[23] C. Nyström, P.G. Karehill, The importance of intermolecular bonding forces and the concept of bonding surface area, in: G. Alderborn, C. Nyström (Eds.), Pharmaceutical Powder Compaction Technology, Marcel Dekker, New York, 1996, pp. 17–53.
[24] K. Ravikumar, S.S. Rajan, V. Pattabhi, Structure of naproxen $C_{14}H_{14}O_3$, Acta Cryst. C41 (1985) 280–282.
[25] Y.B. Kim, H.J. Song, I.Y. Park, Refinement of the structure of (+)-6-methoxy-a-methyl-2-naphthaleneacetic acid, Arch. Pharm. Res. 10 (1987) 232.
[26] Y. Kim, I.Y. Park, W.R. Lah, The crystal structure of naproxen sodium ($C_{14}H_{13}O_3Na$) a non-steroidal antiinflammatory agent, Arch. Pharm. Res. 13 (1990) 166–173.